

Elsevier required licence: © <2019>. This manuscript version is made available under the CC-BY-NC-ND 4.0 license <http://creativecommons.org/licenses/by-nc-nd/4.0/>

The definitive publisher version is available online at

[\[https://www.sciencedirect.com/science/article/pii/S0045653518322604?via%3Dihub\]](https://www.sciencedirect.com/science/article/pii/S0045653518322604?via%3Dihub)

1 **Acid mine drainage treatment by integrated submerged membrane**
2 **distillation –sorption system**

3
4 Seongchul Ryu^a, Gayathri Naidu^a, Md. Abu Hasan Johir^a, Sanghyun Jeong^b, Saravanamuthu
5 Vigneswaran^{a,*}

6 ^a Faculty of Engineering, University of Technology Sydney (UTS), P.O. Box 123, Broadway NSW 2007, Australia²

7 ^b Graduate School of Water Resources, Sungkyunkwan University (SKKU), 2066, Seobu-ro,

8 Jangan-gu, Suwon-si, Gyeonggi-do 16419, Republic of Korea.

9

10 *Corresponding author: Tel +61-2-9514-2641; Fax +61-2-9514-2633; Email: Saravanamuth.Vigneswaran@uts.edu.au

11

12

13 **Abstract**

14 Acid mine drainage (AMD), an acidic effluent characterized by high concentrations of sulfate
15 and heavy metals, is an environmental and economic concern. The performance of an
16 integrated submerged direct contact membrane distillation (DCMD) – zeolite sorption system
17 for AMD treatment was evaluated. The results showed that modified (heat treated) zeolite
18 achieved 26-30% higher removal of heavy metals compared to natural untreated zeolite.
19 Heavy metal sorption by heat treated zeolite followed the order of Fe>Al>Zn>Cu>Ni and the
20 data fitted well to Langmuir and pseudo second order kinetics model. Slight pH adjustment
21 from 2 to 4 significantly increased Fe and Al removal rate (close to 100%) due to a
22 combination of sorption and partial precipitation. An integrated system of submerged DCMD
23 with zeolite for AMD treatment enabled to achieve 50% water recovery in 30 h. The
24 integrated system provided a favourable condition for zeolite to be used in powder form with
25 full contact time in a storing tank. Likewise, heavy metal removal from AMD by zeolite,
26 specifically Fe and Al, mitigated membrane fouling on the surface of the hollow fiber

27 submerged membrane. The integrated system produced high quality fresh water while
28 concentrating sulfuric acid and valuable heavy metals (Cu, Zn and Ni).

29

30 **Keywords**

31 Acid mine drainage, Heavy metal, Integrated process, Submerged membrane distillation,
32 Sorption, Zeolite

33

34 **1. Introduction**

35 The formation of acid mine drainage (AMD) is a natural process attributed to the oxidation of
36 sulfide minerals such as pyrites (Kalin et al., 2006; Mosley et al., 2018). Active and
37 abandoned mines intensifies the formation of AMD due to open pits, mining waste rock,
38 structures and tailings that are exposed to water, air and bacterial activity (Kalin et al., 2006;
39 Mosley et al., 2018; Tolonen et al., 2014). AMD is characterized by low pH and high
40 concentration of sulfate, as well as high concentrations of heavy metals activity (Kalin et al.,
41 2006; Mosley et al., 2018; Tolonen et al., 2014). Nearby water streams are susceptible to
42 AMD infiltration, resulting in discoloration of streams, decrease in pH and accumulation of
43 heavy metals. In Australia, there are a significantly high amount of abandoned mines (more
44 than 50,000 mines) compared to actively operating mines (around 380 mines) (Parbhakar-Fox
45 et al., 2014; Unger et al., 2012). An estimated total land area of 215,000 km² around
46 coastlines and inlands in Australia contain acid sulfate soils attributed to AMD (Fitzpatrick et
47 al., 2009). The long-term impact of AMD contaminant on aquatic organisms, plant growth
48 and human health is a significant concern, which necessitates AMD treatment (Mosley et al.,
49 2018).

50

51 Conventionally, AMD is treated by using alkaline neutralizing chemicals such as caustic soda
52 or limestone, to elevate the pH and precipitate metals (Tolonen et al., 2014). Although
53 efficient, precipitation results in large volumes of sludge containing heavy metals that require
54 safe disposal (Marcello et al., 2008). Various other active and passive remediation
55 approaches such as bioremediation, wetlands, adsorption, phytoremediation are also used to
56 treat AMD (Zhang, 2011; Vasquez et al., 2016; Crane and Sapsford, 2018). In this regard, the
57 uptake of heavy metals by low-cost sorbents are especially promising as a cost effective
58 treatment method for AMD.

59

60 In Australia, naturally occurring zeolites are available in large quantities at relatively low cost
61 (Santiago et al., 2016). A significant advantage of zeolite is its tendency to adsorb cations.
62 The ion exchange affinity of natural and synthetic zeolites for metal extraction from
63 wastewater solution including acid mine drainage has been described by previous studies
64 (Motsi et al., 2009; Rios et al., 2008; Wingfelder et al., 2005). Castle Mountain, Australia
65 produces a natural clinoptilolites (An et al., 2011). The uptake of heavy metals from AMD by
66 Australian natural clinoptilolites may offer a low cost treatment option for AMD. In this
67 regard, a number of approaches are used to enhance the sorption capacity of natural zeolite
68 such as heat treatment, surface and chemical modification (Motsi et al., 2009; Taffarel and
69 Rubio, 2010; Turner et al., 2000). Motsi et al. (2009) reported on the enhanced heavy metal
70 removal of natural zeolite upon microwave and furnace heat treatment. Heat treatment for
71 enhancing the performance of natural zeolite is especially attractive given that it requires no
72 additional chemicals and complex processes.

73

74 Compared to the conventional approach of treat and discharge, more focus is now being
75 placed on achieving water reuse for AMD treatment. Therefore, membrane technologies are

76 becoming favourable AMD treatment options. This is especially reflected by the increase in
77 the implementation of membrane treatment processes such as reverse osmosis (RO) and
78 nanofiltration (NF) at actual mining sites (Aguilar et al., 2016; Ambiado et al., 2017).
79 Although NF and RO do meet good water reuse standards, membrane fouling and low
80 recovery rate remain challenges. In view of this, recent studies are exploring the potential of
81 alternative membrane processes such as electrodialysis, and forward osmosis for AMD
82 treatment. For instance, Martí-Calatayud et al. (2014) reported on the promising capacity of
83 electrodialysis for treating AMD but inorganic membrane precipitation by metals such as iron
84 was a significant drawback. Similarly, Vital et al. (2018) explored the feasibility of using
85 forward osmosis with NaCl as a draw solution for treating AMD. Although FO was able to
86 achieve more than 98% rejection of ions, the phenomenon of reverse salt flux and dilution of
87 draw solution were major limitations.

88
89 Alternatively, membrane distillation (MD), a thermal based membrane process, has shown
90 promising potential for treating acid based wastewater from metal pickling industry
91 (Tomaszewska et al., 2001), and concentrating various types of acid including sulfuric acid
92 from AMD (Kesieme et al., 2012; Tomaszewska and Mientka, 2009). The suitability of MD
93 for concentrating acid is attributed to its capacity to achieve high rejection of non-volatile
94 compounds with up to 90% water recovery ratio, producing good quality fresh water by using
95 vapor pressure difference as its driving force. Additionally, MD requires minimal electrical
96 energy requirement compared to pressure operated systems such as RO and NF while the low
97 thermal requirement (40 – 80 °C) can be met by alternative thermal sources such as solar or
98 waste heat (Khayet, 2013). MD offers a promising potential for achieving near zero liquid
99 discharge for small scale treatment such as AMD (Naidu et al., 2014; Naidu et al., 2017).

100

101 Direct contact MD (DCMD) is the most studied MD configuration due to its simplicity
102 (Naidu et al., 2017). A number of operating approaches has been considered to improve the
103 performance of DCMD. One such approach is using submerged DCMD, in which the
104 membrane module is submerged directly into the feed solution tank (Choi et al., 2017). This
105 configuration enables to achieve a compact system with reduced heat losses, attributed to the
106 elimination of feed recirculation and reheating. Another promising aspect of submerged
107 DCMD is its flexibility to be used as an integrated single system such as a submerged
108 membrane–sorption system (Naidu et al., 2018). The application of submerged DCMD as an
109 integrated single system for heavy metal removal while simultaneously producing fresh water
110 and concentrating AMD has yet to be explored.

111

112 The focus of this study is to evaluate the performance of (i) Australia’s natural and modified
113 (heat treated) zeolite for heavy metal removal from AMD (ii) submerged DCMD for
114 producing water for reuse from AMD and (iii) integrated submerged DCMD – sorption
115 system for simultaneously removing heavy metals and producing water for reuse from AMD.

116

117 **2. Material and methods**

118 **2.1 Acid mine drainage solution**

119 A model acid mine drainage (AMD) solution was prepared based on AMD characteristics
120 from actual mining sites reported by previous studies (Caraballo et al., 2009; Contreras et al.,
121 2015) (**Table 1**). The model solution was prepared by dissolving analytical grade CaSO₄,
122 MgSO₄·(3H₂O), NaOH, FeO(OH), Fe(SO₄)·7H₂O, ZnSO₄·7H₂O, CuSO₄·5H₂O,
123 Al₂(SO₄)₃·18H₂O and Ni(NO₃)₂·6H₂O (Sigma-Aldrich and Thermo Fisher Scientific) in
124 Milli-Q water. The solution pH was adjusted using 10 M of concentrated sulfuric acid
125 (H₂SO₄) (10 M). The pH and total dissolved solids (TDS) contents of the AMD solution was
126 detected by a portable multimeter (HQ40d, HACH, US). Inductively coupled plasma-mass
127 spectrometry (ICP-MS, Agilent 7900, US) was used to analyse the cation value in AMD.
128 Sulfate concentration was measured by ion chromatography (IC, 790 Personal IC, Metrohm,
129 Switzerland).

130

131 **Table 1** Characteristics of synthetic AMD

Parameters	Values	Unit
pH	2.0 ± 0.2	-
TDS	6.35	g/L
Ca	170	mg/L
Mg	220	mg/L
Na	50	mg/L
Fe	340	mg/L
Zn	120	mg/L
Cu	90	mg/L
Al	150	mg/L

Ni	3.5	mg/L
SO ₄	4.3	g/L

132

133 **2.2 Zeolite**

134 **2.2.1 Natural zeolite**

135 The performance of natural Australian zeolite sorbent in powder form (particle size < 75 µm)
 136 for heavy metal removal from AMD solution was evaluated. The mineral composition (as
 137 supplied by Castle Mountain, NSW, Australia) is listed in **Table 2**. This natural zeolite with a
 138 bulk density of is 2.7 g/cm³ is mainly encompassed of clinoptilolite (~85 wt%) with minor
 139 percentages of quartz and mordenite (~15 wt%).

140

141 **2.2.2 Heat treated zeolite**

142 Heat treatment method was used to potentially enhance the performance of natural zeolite
 143 (Motsi et al., 2009; Turner et al., 2000). Heat treatment was chosen as it requires no
 144 additional chemicals and complex modification process. Heat treatment was carried out by
 145 placing an appropriate amount of powder form natural zeolite in a ceramic dish. The ceramic
 146 dish was then placed into preheated air atmosphere muffle furnace (Labec Laboratory Pty
 147 Ltd, NSW, Australia). Heat treatment was carried out at four different temperatures of 300,
 148 400, 500 and 600 °C for 24 h. Upon heat treatment, the zeolite sorbents were stored in air
 149 tight containers in a desiccator.

150

151 **Table 2** Natural zeolite chemical contents

Chemical content	wt.%
SiO ₂	71.81
Al ₂ O ₃	12.10

CaO	2.60
Na ₂ O	2.33
Fe ₂ O ₃	1.14
K ₂ O	0.90
MgO	0.65
TiO ₂	0.22
MnO	0.03
SrO	0.22
P ₂ O ₅	<0.01

152

153 **2.3 Zeolite characteristics**

154 **2.3.1 Surface area and pore width distribution**

155 Nitrogen adsorption test was used to determine the Brunauer–Emmett–Teller (BET) specific
156 surface area and the Barrett–Joyner–Halenda (BJH) pore width distribution of the natural and
157 heat treated zeolite samples. Nitrogen adsorption test was measured with a Micrometrics
158 ASAP 2020 HD analyzer using low temperature, per the procedure of ISO 9277 and ISO
159 15901-2.

160

161 **2.3.2 Crystal structure**

162 X-ray diffraction (XRD) (Siemens D5000 diffractometer operating with Cu-K α radiation
163 source) was used to detect the crystal structure of zeolite (natural and heat treated samples) in
164 powder form. A rotating sample stage was used to scan the samples at 2 θ angular range of 10
165 to 80° in room temperature.

166

167 **2.3.3 Surface morphology and element contents**

168 A scanning electron microscopy (SEM) ((Zeiss Supra 55VP Field Emission) was used to
169 analyse the zeolite surface characteristics (before and upon sorption). The SEM was
170 integrated with energy dispersive X-ray spectroscopy (EDX) (15kV accelerating voltage) in
171 order to analyse the element contents in zeolite.

172

173 **2.3.4 Influence of pH and surface charge**

174 The pH influence on heavy metal sorption by zeolite was determined by varying the pH of
175 AMD solution from 2 to 5. The initial pH of the solution was adjusted using 10 M of H₂SO₄
176 and NaOH. Zeolite (10 g/L) was placed in beakers with 100ml AMD solution. The pH of the
177 initial solutions were varied. The flasks were kept suspended for 12 h in a shaker (120 rpm) at
178 ambient temperature (24 °C). The initial and final pH of the AMD solution in the beakers
179 were recorded.

180

181 Zeolite surface charge was determined using zeta potential measurement. For this purpose,
182 zeolite (1 g/L) placed in beakers with 100ml AMD solution. The pH of the initial solutions
183 were varied from 1 – 9. The flasks were kept suspended for 12 h in a shaker (120 rpm) at
184 room temperature (24 ± 1 °C). Zetasizer (nano instrument ZS Zen3600, UK) was used to
185 analyse the zeolite surface charge.

186

187 **2.4 Sorption study**

188 **2.4.1 Equilibrium**

189 For equilibrium sorption in batch study, zeolite with varying doses ranging from 0.10 – 15
190 g/L was added to beakers containing 100 ml of AMD solutions. The beakers were kept
191 suspended for 12 h in a shaker (120 rpm) at room temperature (24 ± 1 °C) to achieve
192 equilibrium sorption. The solution pH was maintained at 2.0 ± 0.2 to evaluate the

193 performance of zeolite in actual acidic AMD condition and to ensure no precipitation of
194 heavy metal occurred at increased pH. The concentration of heavy metals (Fe, Al, Zn, Cu and
195 Ni) in AMD solution before and after sorption was analysed using ICP-MS. Q_e (mg/g),
196 equilibrium sorption capacity, was represented by Eq. (1):

197

$$198 \quad Q_e = \frac{V(C_i - C_e)}{M} \quad (1)$$

199

200 V (L)= solution volume and M (g) = sorbent mass. C_i and C_e are the concentrations of the
201 heavy metals at initial and equilibrium, respectively.

202

203 Isotherm models (Langmuir and Freundlich) were used to analyse the equilibrium sorption
204 data as below:

205

$$206 \quad \text{Langmuir isotherm: } Q_e = \frac{Q_m b C_e}{1 + b C_e} \quad (2)$$

207

$$208 \quad \text{Freundlich isotherm: } Q_e = K C_e^{1/n} \quad (3)$$

209

210 in which, Q_m (mg/g) is the sorption at maximum capacity and b (L/mg) is the Langmuir
211 constant in relation to the affinity of site binding. K ($\text{g}^{1-n} \text{L}^n \text{g}^{-1}$) is Freundlich constant which
212 relates to the affinity of the sorption and $1/n$ is a dimensionless parameter related to surface
213 heterogeneity.

214

215 **2.4.2 Kinetics**

216 Sorption kinetics was conducted in beakers containing AMD solution (100 ml) and zeolite at
217 a dose of 10 g/L. The solution pH was maintained at 2.0 ± 0.2 . The beakers were kept
218 suspended in a shaker (120 rpm) at room temperature (24 ± 1 °C). At varying time from 0.08
219 h up to 24 h, the solutions in the beaker was collected and the metal contents were measured.
220 The kinetic sorption data were computed using kinetic models (pseudo-first and second
221 order) as presented by Eq. (4) and (5):

222

223 Pseudo first order: $\frac{dQ_t}{dt} = k_1(Q_e - Q_t)$ (4)

224

225 Pseudo second order: $\frac{dQ_t}{dt} = k_2(Q_e - Q_t)^2$ (5)

226

227 The parameters, k_1 and k_2 , represent the adsorption rate (h^{-1}), Q_t and Q_e are the sorption
228 capacity (mg/g) at time t and at equilibrium, respectively.

229

230 **2.5 Submerged direct contact membrane distillation**

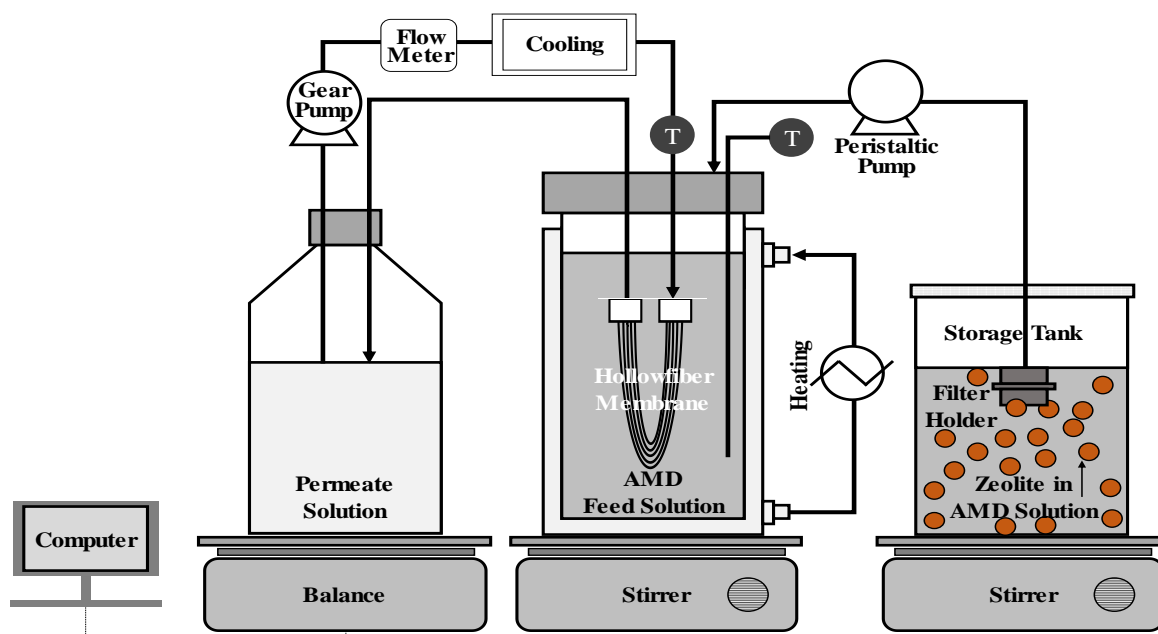
231 A direct contact membrane distillation (DCMD) in submerged condition was used in this
232 study to evaluate the potential of water reuse from AMD solution (**Fig. 1**). The set-up
233 consists of a double wall feed tank containing AMD solution with a submerged hollow fiber
234 membrane made of polyvinylidene fluoride (PVDF). The membrane was obtained from
235 Econity, Republic of Korea) (Choi et al., 2017; Yao et al., 2018). The membrane pore size,
236 inner and outer diameters, wall thickness, and contact angle are 0.1 μm , 0.7 mm and 1.2 mm,
237 250 μm and $106 \pm 2^\circ$ respectively. The membrane module was made of 18 fibers with 0.2 m
238 length (active membrane area of 0.0136 m^2).

239

240 The outer wall of the double wall feed tank was circulated with heated water connected to a
241 heating system, enabling to maintain a AMD feed solution temperature of 55.0 ± 0.5 °C. The
242 permeate solution was maintained at 22 ± 0.5 °C using a cooling system. A gear pump was
243 used to circulate the permeate solution at a flow rate of 0.8 L/min. The increase in permeate
244 volume in the permeate tank was recorded over time using an electronic balance. This is used
245 to compute the permeate flux over time. AMD solution was kept at constant volume of 0.9 L
246 in the feed tank by replenishing fresh AMD feed solution (from a storage tank) at the same
247 rate as the permeate production rate using a peristaltic pump.

248

249 This study evaluated the potential of combining submerged DCMD and zeolite into a single
250 integrated process. For the integrated submerged DCMD–sorption process, AMD solution
251 (pretreated with zeolite) was placed in the feed tank. Meanwhile in the storage tank, zeolite at
252 a predetermined dose was kept suspended at a rate of 120 rpm (as per the batch sorption
253 study) in 1.5 L of AMD solution. This enabled heavy metal removal by zeolite from AMD
254 solution in the storage tank. A filter holder containing glass fiber membrane (Filtech,
255 Australia) with a pore size of 1.1 μm was placed at the top of the holding tank to filter the
256 used zeolite, ensuring only pretreated AMD solution enters the feed tank.



258

259 **Fig. 1.** Set-up of integrated submerged DCMD – sorption system260 **2.5.1 Membrane analysis**

261 The morphology and element composition on the surface of the used and virgin membranes
 262 were analysed using SEM-EDX at a voltage of 15 kV as per the details mentioned in Section
 263 2.3.3. The hydrophobicity of the virgin and used membranes were evaluated by measuring
 264 the water contact angle of the membrane using a goniometer (Theta Lite, Biolin Scientific,
 265 Sweden). Measurements were duplicated at different location of the membrane and the
 266 average value was used for this study.

267

268 **3. Results and discussion**269 **3.1 Performance of natural and modified (heat treated) zeolite**

270 The sorption capacity of natural and modified (heat treated) zeolite was tested for heavy
 271 metal removal from AMD. Higher heavy metal removal was achieved with heat treated
 272 zeolite compared to natural untreated zeolite (**Table 3**). The removal of heavy metals
 273 increased from 1 – 12% with natural zeolite by up to 30 – 38% upon heating (500 °C).

274 Heating may have removed water on the surface as well as internal channels of the natural
 275 zeolite, resulting in vacant channels which enhances heavy metal sorption rate, as reported by
 276 previous studies (Ohgushi and Nagae, 2003; Turner et al., 2000). However, heavy metal
 277 removal by zeolite minimally improved beyond 500 °C of heating. This trend could be
 278 attributed to characteristics change of zeolite upon heat treatment.

279

280 **Table 3** Performance of natural and heat treated zeolite with AMD solution (sorbent dose 5.0
 281 ± 0.2 g/L, pH 2.0 ± 0.2).

Sorbent type	Heavy metal removal (%)				
	Fe	Al	Zn	Cu	Ni
Natural zeolite	12.8 \pm 0.9	1.1 \pm 0.2	9.4 \pm 1.4	11.2 \pm 0.7	10.8 \pm 1.1
Heat treated zeolite					
300 °C	17.9 \pm 1.6	15.7 \pm 0.8	15.6 \pm 2.4	17.1 \pm 1.5	15.9 \pm 2.0
400 °C	25.3 \pm 2.2	26.1 \pm 1.3	21.1 \pm 2.0	22.8 \pm 1.2	19.7 \pm 1.9
500 °C	34.9 \pm 2.7	36.3 \pm 2.7	29.3 \pm 2.3	31.3 \pm 1.9	21.1 \pm 1.3
600 °C	31.0 \pm 2.5	30.8 \pm 2.4	27.0 \pm 2.3	29.1 \pm 2.1	20.0 \pm 2.9

282

283 3.1.1 Characteristics of zeolite

284 3.1.1.1 Surface area and pore width distribution

285 The surface area (BET) and pore width (BJH) of natural zeolite was 14.5 m²/g and 147.59 Å.
 286 The surface area and pore width of zeolite showed an increasing trend with heat treatment up
 287 to 500 °C (**Table 4**). This implies that thermal heating contributed towards the activation of
 288 zeolite surface and possible removal of water (Akdeniz and Ülkü, 2007; Ohgushi and Nagae,
 289 2005). In turn, metal removal increased (**Table 3**). On the other hand, the slightly lower
 290 surface area and pore width at 600 °C compared to 500 °C could explain the minimal
 291 changes in heavy metal removal above 500 °C (**Table 3**).

292

293 The results showed that heat treatment of zeolite at 500 °C was optimum to enhance its
294 performance. Based on these results, 500 °C heat treated zeolite in powder form was used for
295 all further experiments.

296

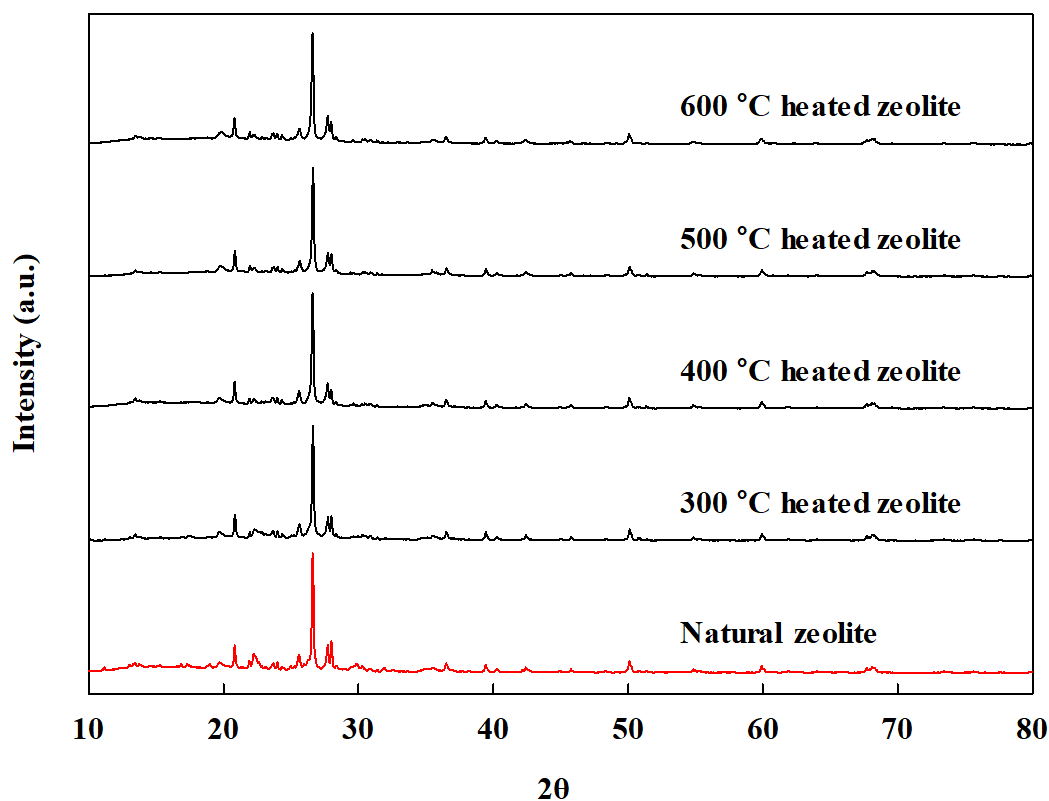
297 **Table 4** Surface area and pore width of natural and heat treated zeolite.

Sorbent type	BET Surface area (m ² /g)	BJH Pore width (Å)
Natural zeolite	14.5	147.6
Heat treated zeolite		
300 °C	14.8	147.5
400 °C	15.0	148.2
500 °C	16.2	150.9
600 °C	14.9	147.9

298

299 3.1.1.2 Crystal structure

300 The XDR spectra (**Fig. 2**) showed similar diffraction pattern for natural and heat treated
301 zeolite. This affirmed that heat treatment did not change the crystal structure. Further, the
302 XRD spectra also established that the natural Australian zeolite used in this study
303 corresponded to that of the structure of clinoptilolite, as reported by previous papers (Nguyen
304 et al., 2015; Naidu et al., 2018).

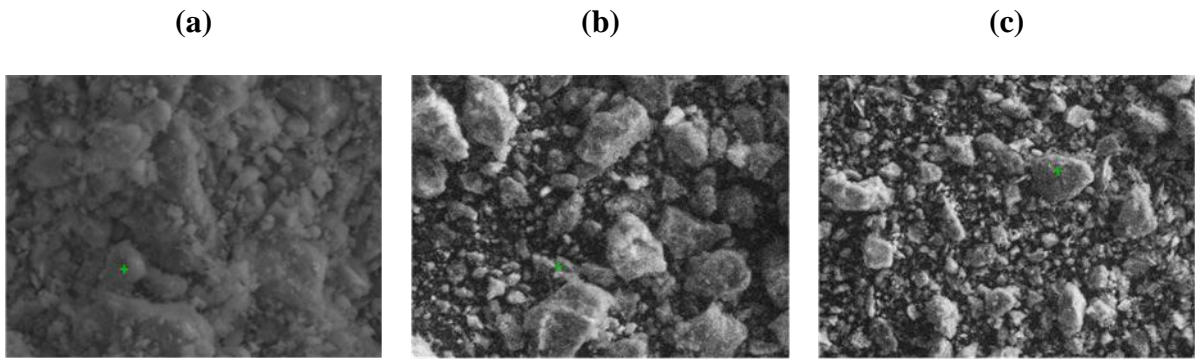


305
 306 **Fig. 2.** XRD peaks of natural and heat treated zeolite

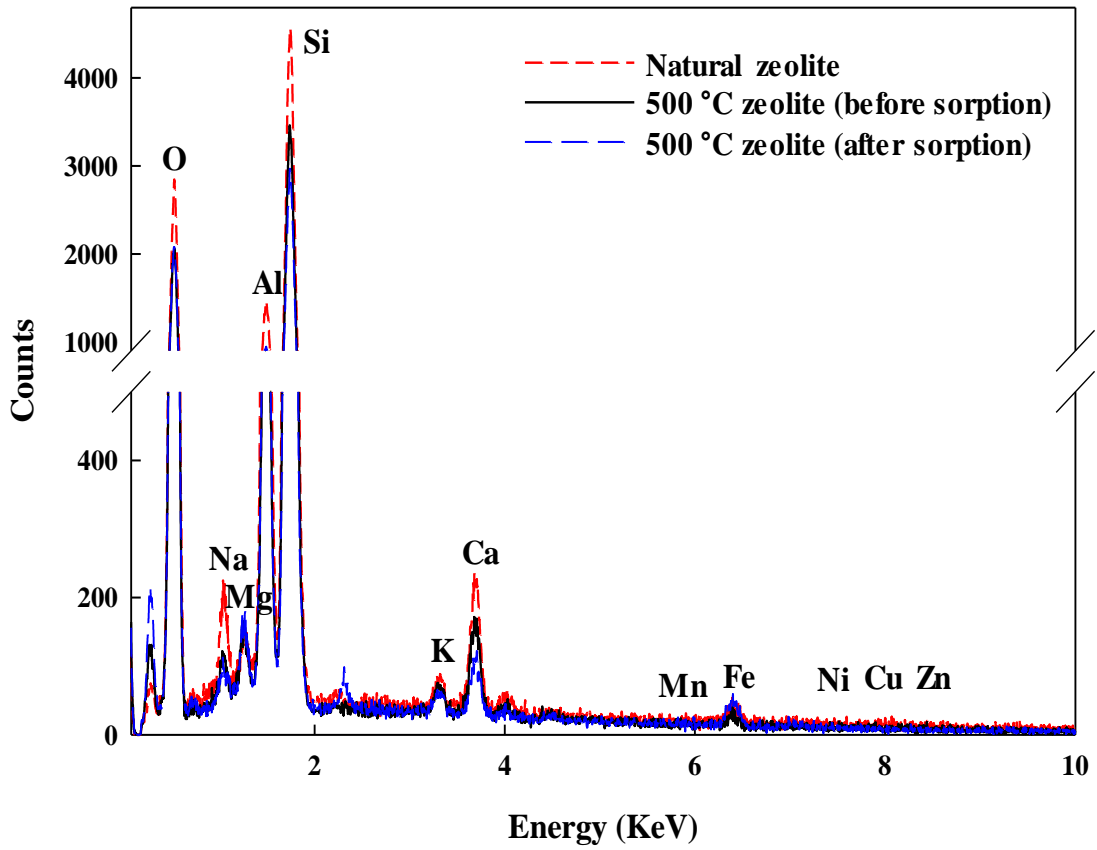
307
 308 **3.1.1.3 Surface morphology and element contents**

309 The SEM images showed the heterogeneous condition of the zeolite (**Fig. 3**). No significant
 310 morphology changes were observed between the natural and heat treated zeolites.

311
 312 The EDX established Si, O, K, Al, Mg, Na, Fe and Ca as the main element peaks in all
 313 zeolite structure (**Fig. 4**). The slight decrease of O atomic content from 67.52 in the natural
 314 zeolite to 66.61% upon heat treatment could be due to the removal of water in the internal
 315 channels (**Table 5**). The EDX analysis of heat treated zeolite (after sorption of heavy metals
 316 from AMD) showed reduction in Si, Na, Ca and K. Meanwhile the increase of Fe and Al as
 317 well as the presence of Cu, Zn and Ni establish the heavy metal sorption from AMD.



318 **Fig. 3.** SEM images of (a) natural untreated zeolite and 500 °C heat treated zeolite (b)
 319 unused/before sorption and (c) after heavy metal sorption



320
 321 **Fig. 4.** EDX results of natural and 500 °C heat treated zeolite (before and after heavy metal
 322 sorption).
 323
 324

325 **Table 5** EDX results of natural and 500 °C heat treated zeolite

Element	% atomic ratio		
	Natural zeolite	500 °C heat treated zeolite	
		Before sorption	After sorption
O	67.52	66.61	66.86
Si	20.95	24.68	22.56
Al	7.61	5.25	6.65
Fe	0.70	0.61	1.27
Ca	1.63	1.41	1.05
Mg	0.27	0.62	0.81
K	0.28	0.30	0.25
Na	1.06	0.54	0.39
Ni			0.10
Cu			0.04
Zn			0.02

326

327 **3.1.2 Equilibrium sorption**

328 **3.1.2.1 Isotherm**

329 Heavy metal sorption from AMD solution with 500 °C heat treated zeolite was computed
 330 with Langmuir and Freundlich sorption isotherm (**Fig. S1** and **Table 6**).

331

332 The data satisfactorily fitted to Langmuir sorption isotherm ($R^2 = 0.87 - 0.98$) compared to
 333 the Freundlich sorption isotherm ($R^2 = 0.79 - 0.89$). Similarly, a number of studies on zeolite
 334 performance for heavy metal removal indicated the suitability of Langmuir isotherm (Motsi
 335 et al., 2009; Nguyen et al., 2015; Qiu and Zheng, 2009). Based on the sorption isotherm, heat
 336 treated zeolite capacity for heavy metal removal from AMD followed the order of

337 Fe>Al>Zn>Cu>Ni. Poor removal of Ni by a zeolite could be due to the high stability of its
 338 aqueous complex (Mondale et al., 1995).

339
 340 The better Langmuir fitting indicated that the sorption sites were homogeneous with
 341 monolayer sorption coverage. However, not all the heavy metals achieved a fitting of R^2
 342 above 0.95. This could be attributed to the mixed metals present at different concentrations in
 343 AMD (**Table 1**) resulting in competition of sorption. Nguyen et al (2015) compared the
 344 Langmuir fitting of heavy metal removal by zeolite and observed lower Langmuir capacity
 345 and fitting for each metal in a mixed metal solution compared to individual metal solution.

346
 347 **Table 6** Isotherm data (Langmuir and Freundlich) for heavy metal sorption from AMD
 348 solution at pH 2.0 ± 0.2 using 500 °C heat treated zeolite.

Heavy metal	Langmuir			Freundlich		
	Q_{max} (mg/g)	K_L (L/mg)	R^2	n	K_F (mg/g)(L/mg) ^{1/n}	R^2
Fe	62.11	0.031	0.97	3.20	9.73	0.89
Al	44.64	0.072	0.90	1.40	1.34	0.83
Zn	39.06	0.114	0.98	3.65	10.38	0.85
Cu	36.10	0.075	0.95	2.67	6.11	0.81
Ni	1.09	1.326	0.91	1.96	0.62	0.90

349
 350

351 3.1.2.2 Kinetics

352 Sorption of all heavy metals from AMD solution by 500 °C heat treated zeolite increased
353 with time up to 12 hours and reached equilibrium at approximately 20 h. From the uptake
354 curves in **Fig. S2**, it is evident that the rate of sorption was initially fast (within 4 h) and was
355 gradually slow when approaching equilibrium. Kinetic experiment of heavy metal sorption
356 was fitted to pseudo first and second order models (**Fig. S2** and **Table 7**). The experimental
357 data was well matched to both pseudo first order ($R^2 = 0.94 - 0.99$) and pseudo second order
358 ($R^2=0.99$). The calculated Q_e in both cases were almost similar to the experimental values of
359 Q_e .

360

361 **Table 7** Pseudo first and second order kinetic parameters for heavy metal sorption from
362 AMD solution at pH 2.0 ± 0.2 using 500 °C heat treated zeolite (dose = 10 ± 0.2 g/L)

Heavy metals	Q_e (exp) (mg/g)	Pseudo first order			Pseudo second order		
		Q_e (pre) (mg/g)	k_1 (hr ⁻¹)	R^2	Q_e (pre) (mg/g)	k_2 (g/mg/hr)	R^2
Fe	11.95	11.73	1.45	0.98	12.87	0.04	0.99
Al	6.07	6.11	2.06	0.99	6.27	0.20	0.99
Zn	3.89	3.65	1.48	0.94	4.20	0.11	0.99
Cu	3.15	2.98	1.57	0.95	3.36	0.16	0.99
Ni	0.11	0.10	1.55	0.95	0.11	5.17	0.99

363

364 3.1.3 Influence of sorbent dose and pH

365 Increased heavy metal removal was observed with higher zeolite dose (**Fig. 5a**). The reducing
366 trend of Al removal, especially above 10 g/L zeolite may be attributed to Al leaching out
367 from the zeolite structure that contain around 12 wt% Al as Al₂O₃ (**Table 1**).

368

369 **3.1.3.1 Ion exchange mechanism**

370 Above zeolite dose of 10 g/L onwards, insignificant changes in heavy metal removal was
371 observed. This is due to the decline in the remaining ion concentration in solution with
372 increasing sorbent dose (Al-Haj and Ribhi, 1997). The uptake of heavy metal cations by
373 zeolite has been well established as an exchange mechanism between the cations present in
374 the solution and cations in the zeolite framework, mainly Na and Ca (Nguyen et al., 2015;
375 Qiu and Zheng, 2009). The ion exchange mechanism suggest that zeolite may be more
376 selective to monovalent cations. In this scenario, AMD solution (pH 2) contain high H ions
377 and zeolite may preferentially adsorb monovalent H ions from the solution to divalent heavy
378 metals (Sprynsky et al., 2006). This could also explain the increase in the pH of AMD
379 solution from 2.0 to 2.4 upon sorption. Thus, even as the dose of zeolite was increased, heavy
380 metal removal rate remained low in the range of 35 to 40%.

381

382 **3.1.3.2 Electrostatic sorption**

383 Apart from the ion exchange mechanism, electrostatic sorption, which is the attraction of
384 positively charged metal cations towards negatively charged zeolite surfaces, play an
385 important role in influencing the uptake of heavy metals. Based on the zeta potential analysis,
386 the zeolite surface charge showed a trend of increasing negativity from -11 mV to -30 mV as
387 the pH of the solution was increased from 1 to 9 (**Fig. 5b**). Previous studies on natural zeolite
388 characteristics reported similar observations of higher negative surface charge as the solution
389 pH was increased (Englert and Rubio, 2005; Nguyen et al., 2015). Increased negative surface
390 charge of zeolite enhances the sorption tendency onto cation metals through electrostatic
391 sorption (outer sphere mechanism). The results of the zeta potential indicated the significant
392 role of pH for improving metal removal from AMD.

393

394 **3.1.3.3 Partial precipitation**

395 In this study, a pH increase from 2 to 5, significantly increased the removal of Fe and Al by
396 close to 100% (**Fig. 6**). Previous AMD studies have highlighted that, at higher pH, removal
397 of Fe and Al is attributed to the combination of sorption and partial precipitation (Motsi et al.,
398 2009; Wingenfelder et al., 2005). The high precipitation affinity of Fe and Al is due to the
399 low solubility limit of both these metals at pH above 4.

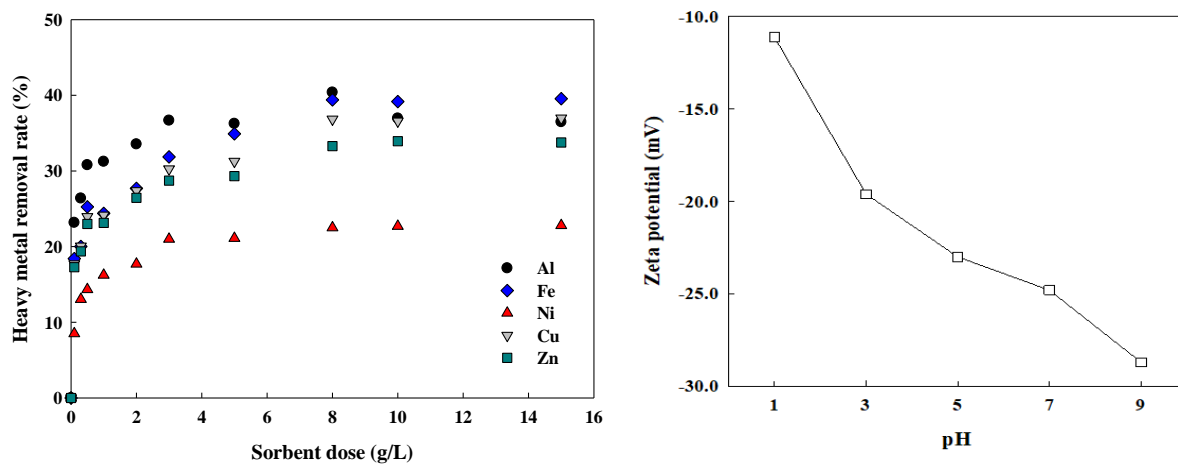
400

401 Meanwhile, varying the pH from 2 to 5 only marginally improved the removal rate of Zn, Cu,
402 and Ni. This result was contrary to a number of zeolite studies that reported on the increase in
403 heavy metal removal rate at higher pH (Alvarez-Ayuso et al., 2003; Moreno et al., 2001;
404 Motsi et al., 2009). Apart from heavy metals, the AMD solution used in this study contained
405 Na and Ca that could have played a competitive role in minimizing the pH effect. Similarly,
406 Wingenfelder et al (2005) reported on the poorer removal of heavy metals namely Cd and Zn
407 in the presence of Ca.

408

409 Overall the results showed that modified (500 °C heat treated) zeolite in powder form
410 enabled to remove heavy metals from AMD attributed to a combination of ion exchange,
411 electrostatic sorption and partial precipitation. Nevertheless, it is a challenge to use the
412 powdered form zeolite in ion exchange filter columns (Naidu et al., 2018). For this purpose,
413 the potential of an integrated system, submerged DCMD with zeolite was evaluated in the
414 subsequent section.

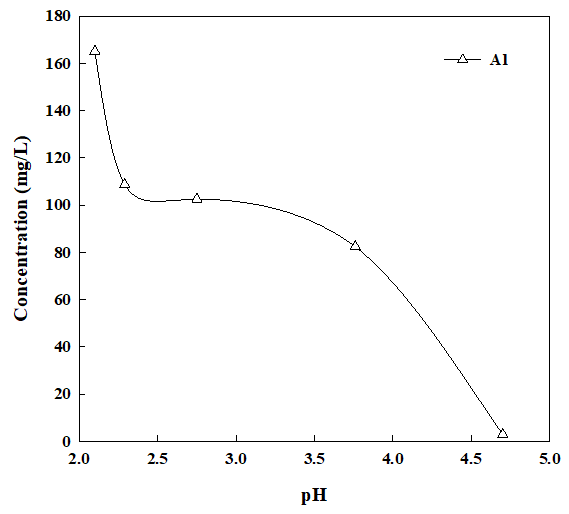
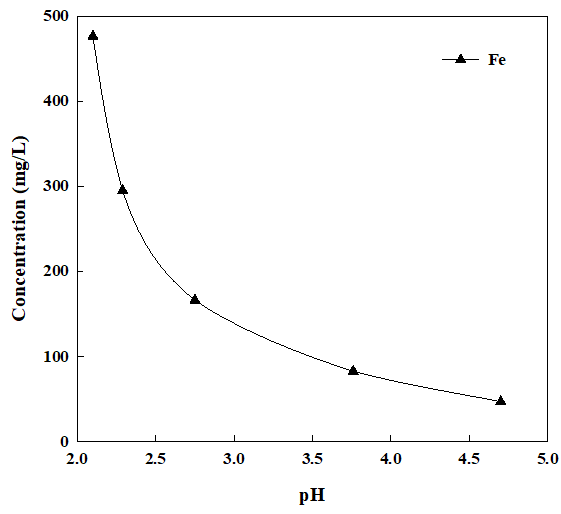
415



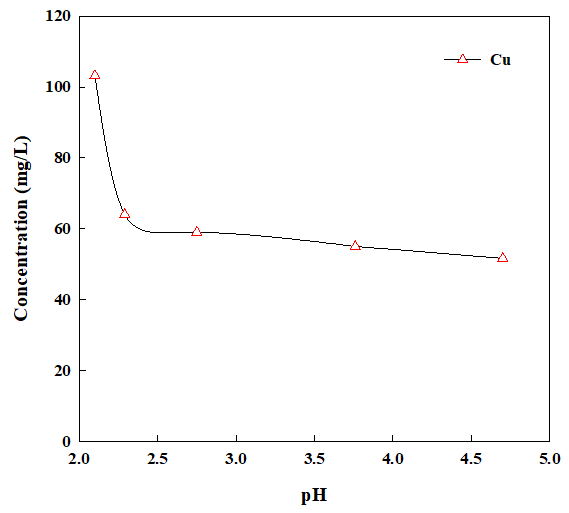
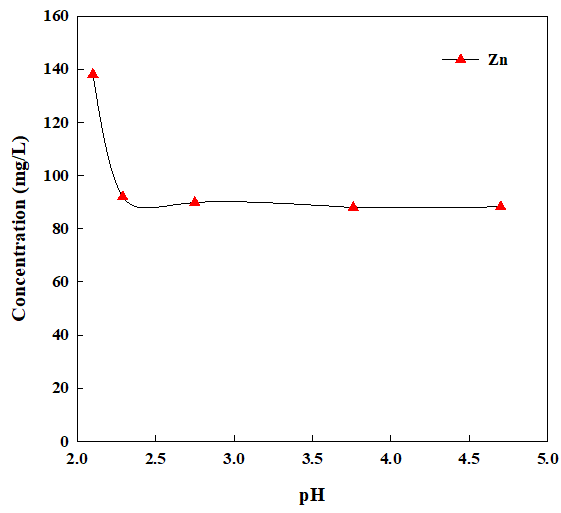
416 **Fig. 5.** 500 °C heat treated zeolite (a) heavy metal removal as a function of sorbent dose (pH
 417 2.0 ± 0.2) (b) zeta potential as a function of pH (dose = 1.0 ± 0.2 g/L, 10⁻³ M KCl as
 418 electrolyte).

419

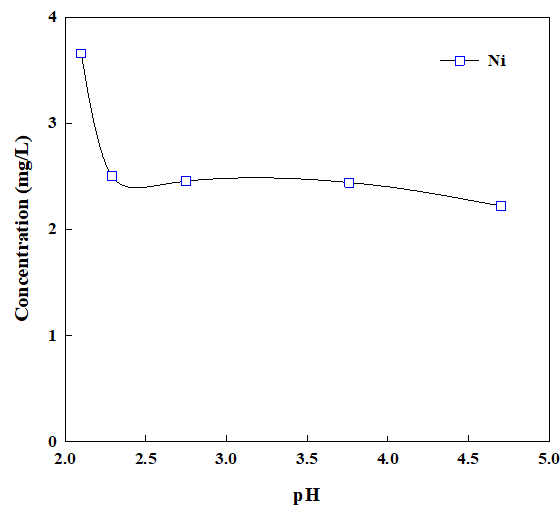
420



421



422



423

424

425 **Fig. 6.** Influence of pH on heavy metal removal from AMD solution with 500 °C heated

426 zeolite (dose = 10 ± 0.2 g/L)

427 **3.2 Performance of submerged DCMD**

428 The potential of achieving good quality water for reuse was evaluated using submerged
429 DCMD.

430

431 **3.2.1 Permeate flux and quality**

432 An initial permeate flux of 2.5 ± 0.2 LMH was achieved (Choi et al., 2018) and the flux
433 remained stable throughout the operation duration (30 h), enabling to achieve 50% water
434 recovery (**Fig. 7**). The initial AMD solution (TDS of 6.4 g/L) was concentrated by 2 times
435 (TDS of 12.9 g/L). Meanwhile, the concentration of permeate solution remained low (TDS
436 less than 0.01 g/L). However, the sulfate concentration in the permeate solution increased
437 significantly from 0.13 mg/L to 50 mg/L.

438

439 **3.2.2. Membrane analysis**

440 Visible brown deposition (resembling iron oxides) was observed on the used membrane (**Fig.**
441 **8b**) compared to the virgin membrane (**Fig. 8a**). SEM-EDX analysis revealed Fe, S and Al
442 deposition on the membrane. The presence of Fe and Al on the membrane could be attributed
443 to the high precipitation affinity of these metals at increased concentration under thermal
444 condition (Gryta, 2007). The precipitated metals predominantly deposited on the membrane
445 surface and was loosely attached to the surface. It is likely that the deposition only partially
446 blocked the membrane pores, and therefore, a stable permeate flux was maintained
447 throughout the operation duration. Nevertheless, the contact angle of the used membrane
448 ($68.6 \pm 0.8^\circ$) reduced by 38 – 40% compared to the virgin membrane ($109.5 \pm 0.5^\circ$),
449 suggesting that the Fe deposition resulted in the reduction of membrane hydrophobicity and
450 partial wetting of sulfate ions.

451

452 **3.3 Performance of integrated submerged DCMD-sorption**

453 An integration of zeolite with submerged DCMD (**Fig. 1**) offers the potential for improving
454 the performance of both processes in a single system. The integrated system enable zeolite to
455 be used in fine powder form with long contact time (more than 24 h) when kept suspended in
456 a storage tank. In return, the heavy metal removal by 500 °C heat treated zeolite (dose = 10.0
457 \pm 0.2 g/L) at pH 4 will ensure minimal Fe and Al deposition onto the membrane during the
458 submerged DCMD process.

459

460 **3.3.1 Permeate flux and quality**

461 The integrated submerged DCMD-sorption system showed similar flux pattern as the
462 submerged DCMD (**Fig. 7**), indicating that the DCMD performance was not affected by the
463 presence of sorbent in the storage tank. The integrated system enabled to achieve high
464 rejection of all ions, maintaining a permeate TDS of less than 0.01 g/L. The sulfate
465 concentration in the feed solution was increased from 4.2 g/L to around 8.2 g/L, while the
466 sulfate concentration in the permeate solution remained low (less than 0.13-0.15 mg/L).

467

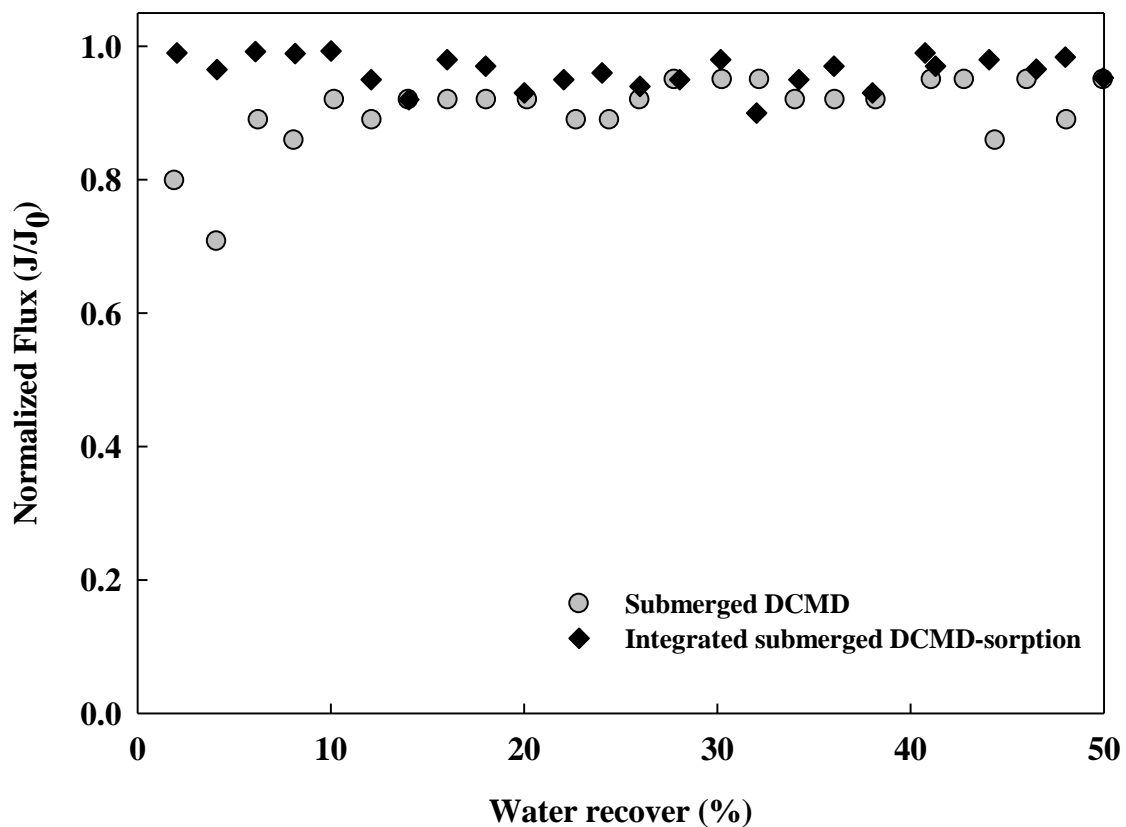
468 **3.3.2. Membrane analysis**

469 The used membrane showed minimal Fe and Al depositions, according to the SEM-EDX
470 analysis (**Fig. 8c**). The contact angle of the used membrane ($99.7 \pm 0.4^\circ$) only reduced
471 slightly by 10% compared to the virgin membrane ($109.5 \pm 0.5^\circ$), suggesting that the
472 membrane hydrophobicity was minimally affected. The membrane analysis established the
473 stability of the membrane to be used to treat acidic AMD solution.

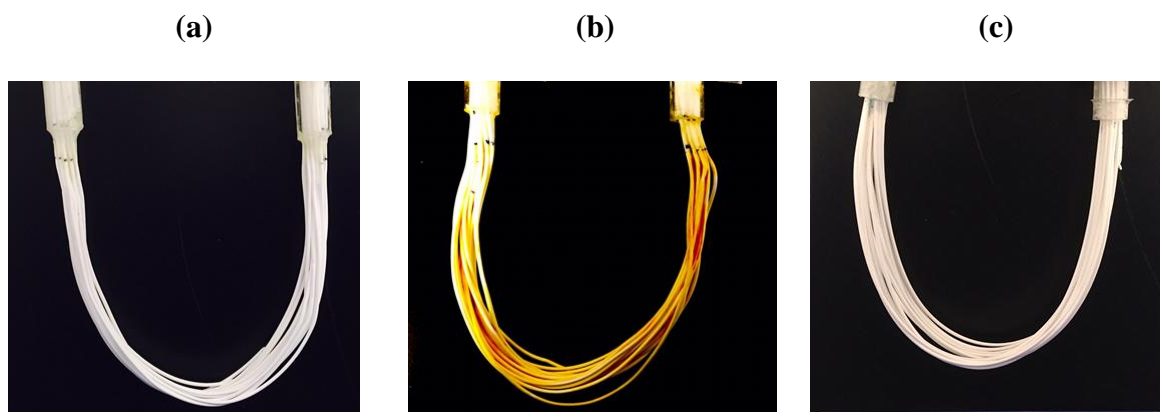
474

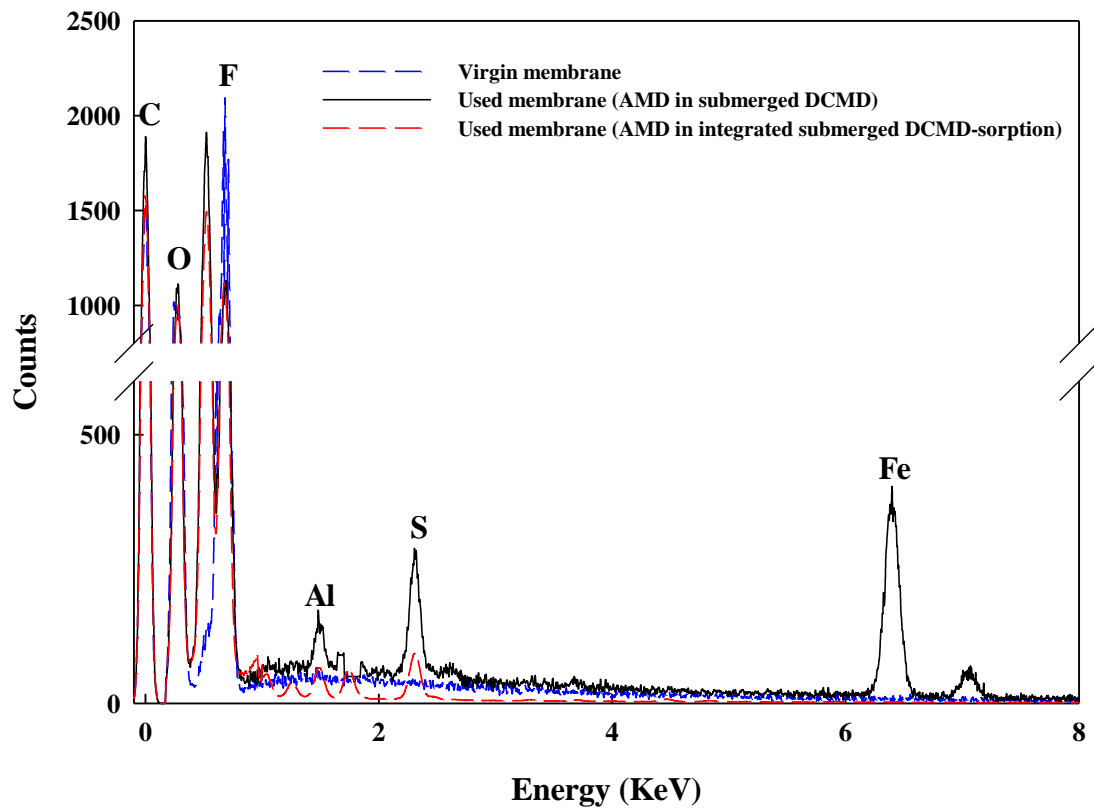
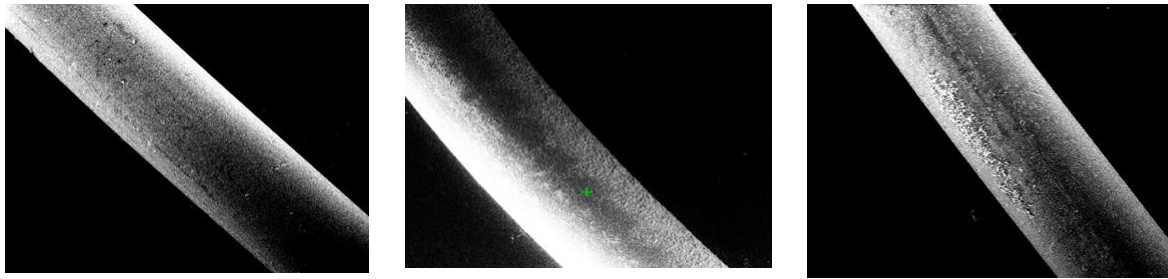
475 Overall, the results indicated the suitability of integrated submerged DCMD-sorption system
476 for producing high quality water with simultaneous uptake of heavy metals by zeolite. The

477 remaining AMD contained concentrated sulfuric acid as well as valuable metals of Cu, Ni
478 and Zn that can be selectively recovered.



479
480 **Fig. 7.** Permeate flux for AMD treatment using submerged DCMD and integrated submerged
481 DCMD –sorption system
482





483 **Fig. 8.** SEM-EDX of hollowfiber membrane (a) virgin (b) used membrane with AMD in
 484 submerged DCMD (c) used membrane with AMD in integrated DCMD-sorption.

485

486 **4. Conclusion**

487 An integrated submerged DCMD – zeolite sorption system for simultaneous removal of
488 heavy metals and fresh water production from AMD was evaluated in this study. The results
489 showed:

- 490 • A simple heat treatment was effective to increase the performance of natural zeolite for
491 heavy metal removal from AMD solution. Heat treatment of natural zeolite at 500 °C
492 enhanced heavy metal removal by 26-30%.
- 493 • The removal affinity for heavy metal was in the order of Fe>Al>Zn>Cu>Ni. The
494 maximum sorption capacity (based on Langmuir Q_{max}) was 62.11, 44.64, 39.96, 36.10,
495 19.80 and 1.09 mg/g respectively.
- 496 • Fe and Al removal was close to 100% with 500 °C heat treated zeolite while 38-40% of
497 Zn, Cu and Ni was achieved.
- 498 • Submerged DCMD enabled to treat AMD solution to achieve 50% water recovery
499 while maintaining a stable flux. Nevertheless, Fe and Al precipitation from
500 concentrated AMD deposited onto the hollow fibre membrane. This reduced the
501 membrane hydrophobicity and caused partial wetting of sulfate ions.
- 502 • An integrated system of submerged DCMD with zeolite sorption provided a favourable
503 condition to use 500 °C heat treated zeolite in powder form with a long contact time (30
504 h) in a submerged tank. In return, the simultaneous uptake of heavy metals by zeolite
505 mitigated membrane fouling. At 50% water recovery, the integrated submerged DMCD
506 – sorption system produced high quality fresh water for reuse while concentrating
507 valuable Cu, Ni and Zn that can be recovered further.

508

509

510

511

512 **Acknowledgements**

513 The authors acknowledge the support received for this study from University of Technology
514 Sydney's (UTS) Early Career Researcher Fund and Centre for Technology in Water and
515 Wastewater, UTS Early Career Researcher program and UTS chancellor's postdoctoral
516 research fellowship

517

518

519 **References**

- 520 Aguiar, A.O., Andrade, L.H., Ricci, B.C., Pires, W.L., Miranda, G.A., Amaral, M.C.S., 2016.
521 Gold acid mine drainage treatment by membrane separation processes: An evaluation of the
522 main operational conditions. *Sep. Purif. Technol.* 170, 360-369.
- 523 Akdeniz, Y., Ülkü, S., 2007. Microwave effect on ion-exchange and structure of
524 clinoptilolite. *J. Porous Mater.* 14(1), 55-60.
- 525 Al-Haj, A.A., Ribhi, E.-B., 1997. Removal of Lead and Nickel Ions Using Zeolite Tuff. *J.*
526 *Chem. Technol. Biot.* 69(1), 27-34.
- 527 Alvarez-Ayuso, E., Garcia-Sanchez, A., Querol, X., 2003. Purification of metal electroplating
528 waste waters using zeolites. *Water Res.* 37(20), 4855-4862.
- 529 Ambiado, K., Bustos, C., Schwarz, A., Bórquez, R., 2017. Membrane technology applied to
530 acid mine drainage from copper mining. *Water Sci. Technol.* 75, 705-715.
- 531 An, W., Swenson, P., Wu, L., Waller, T., Ku, A., Kuznicki, S.M., 2011. Selective separation
532 of hydrogen from C₁/C₂ hydrocarbons and CO₂ through dense natural zeolite membranes. *J.*
533 *Membr. Sci.* 369(1-2), 414-419.
- 534 Caraballo, M.A., Rötting, T.S., Macías, F., Nieto, J.M., Ayora, C., 2009. Field multi-step
535 limestone and MgO passive system to treat acid mine drainage with high metal
536 concentrations. *Appl. Geochem.* 24(12), 2301-2311.
- 537 Choi, Y., Naidu, G., Jeong, S., Lee, S., Vigneswaran, S., 2018. Fractional-submerged
538 membrane distillation crystallizer (F-SMDC) for treatment of high salinity solution.
539 *Desalination* 440, 59-67.
- 540 Choi, Y., Naidu, G., Jeong, S., Vigneswaran, S., Lee, S., Wang, R., Fane, A.G., 2017.
541 Experimental comparison of submerged membrane distillation configurations for
542 concentrated brine treatment. *Desalination* 420, 54-62.

543 Contreras, J.O., Flores, D.P., Gutierrez, P., Crooker, P.C., 2015. Acid Mine Drainage in
544 Chile: An Opportunity to Apply Bioremediation Technology. *Hydrology Current Research*
545 6(3), 1-8.

546 Englert, A.H., Rubio, J., 2005. Characterization and environmental application of a Chilean
547 natural zeolite. *Int. J. Miner. Process.* 75(1-2), 21-29.

548 Crane, R.A., Sapsford, D.J., 2018. Towards “Precision Mining” of wastewater: Selective
549 recovery of Cu from acid mine drainage onto diatomite supported nanoscale zerovalent iron
550 particles. *Chemosphere* 202, 339-348.

551 Fitzpatrick, R.W., Grealish, G., Shand, P., Simpson, S.L., Merry, R.H., Raven, M.D., 2009.
552 Acid sulfate soil assessment in Finniss River, Currency Creek, Black Swamp and Goolwa
553 Channel, South Australia. CSIRO land and water science report 26/09 CSIRO, Adelaide.

554 Gryta, M., 2007. Effect of iron oxides scaling on the MD process performance. *Desalination*
555 216(1-3), 88-102.

556 Kalin, M., Fyson, A., Wheeler, W.N., 2006. The chemistry of conventional and alternative
557 treatment systems for the neutralization of acid mine drainage. *Sci. Total Environ.* 366, 395–
558 408.

559 Kesieme, U.K., Milne, N., Aral, H., Cheng, C.Y., Duke, M., 2012. Novel application of
560 membrane distillation for acid and water recovery from mining waste waters. *International*
561 *Mine Water Association Symposium 2012 Mine Water and the Environment*, Curran
562 Associates Inc., Bunbury, Australia.

563 Khayet, M., 2013. Solar desalination by membrane distillation: Dispersion in energy
564 consumption analysis and water production costs (a review). *Desalination* 308, 89-101.

565 Marcello, R.R., Galato, S., Peterson, M., Riella, H.G., Bernardin, A.M., 2008. Inorganic
566 pigments made from the recycling of coal mine drainage treatment sludge. *J. Environ.*
567 *Manage.* 88(4), 1280-1284.

568 Martí-Calatayud, M.C., Buzzi, D.C., García-Gabaldón, M., Ortega, E., Bernardes, A.M.,
569 Tenório, J.A.S., Pérez-Herranz, V., 2014. Sulfuric acid recovery from acid mine drainage by
570 means of electrodialysis. *Desalination* 343, 120-127.

571 Mondale, K.D., Carland, R.M., Aplan, F.F., 1995. The comparative ion exchange capacities
572 of natural sedimentary and synthetic zeolites. *Miner. Eng.* 8(4), 535-548.

573 Moreno, N., Querol, X., Ayora, C., Pereira, C.F., Janssen-Jurkovicová, M., 2001. Utilization
574 of Zeolites Synthesized from Coal Fly Ash for the Purification of Acid Mine Waters.
575 *Environ. Sci. Technol.* 35(17), 3526-3534.

576 Mosley, L.M., Biswas, T.K., Dang, T., Palmer, D., Cummings, C., Daly, R., Simpson, S.,
577 Kirby, J., 2018. Fate and dynamics of metal precipitates arising from acid drainage
578 discharges to a river system. *Chemosphere* 212, 811-820.

579 Motsi, T., Rowson, N.A., Simmons, M.J.H., 2009. Adsorption of heavy metals from acid
580 mine drainage by natural zeolite. *Int. J. Miner. Process.* 92(1-2), 42-48.

581 Naidu, G., Jeong, S., Choi, Y., Jang, E., Hwang, T.-M., Vigneswaran, S., 2014. Application
582 of vacuum membrane distillation for small scale drinking water production. *Desalination* 354,
583 53-61.

584 Naidu, G., Jeong, S., Choi, Y., Song, M.H., Oyunchuluun, U., Vigneswaran, S., 2018.
585 Valuable rubidium extraction from potassium reduced seawater brine. *J. Clean. Prod.* 174,
586 1079-1088.

587 Naidu, G., Jeong, S., Choi, Y., Vigneswaran, S., 2017. Membrane distillation for wastewater
588 reverse osmosis concentrate treatment with water reuse potential. *J. Membr. Sci.* 524, 565-
589 575.

590 Nguyen, T.C., Loganathan, P., Nguyen, T.V., Vigneswaran, S., Kandasamy, J., Naidu, R.,
591 2015. Simultaneous adsorption of Cd, Cr, Cu, Pb, and Zn by an iron-coated Australian zeolite
592 in batch and fixed-bed column studies. *Chem. Eng. J.* 270, 393-404.

593 Ohgushi, T., Nagae, M., 2003. Quick Activation of Optimized Zeolites with Microwave
594 Heating and Utilization of Zeolites for Reusable Desiccant. *J. Porous Mater.* 10(2), 139-143.

595 Ohgushi, T., Nagae, M., 2005. Durability of Zeolite Against Repeated Activation Treatments
596 with Microwave Heating. *J. Porous Mater.* 12(4), 265-271.

597 Parbhakar-Fox, A.K., Edraki, M., Hardie, K., Kadletz, O., Hall, T., 2014. Identification of
598 acid rock drainage sources through mesotextural classification at abandoned mines of
599 Croydon, Australia: Implications for the rehabilitation of waste rock repositories. *J.*
600 *Geochem. Explor.* 137, 11-28.

601 Qiu, W., Zheng, Y., 2009. Removal of lead, copper, nickel, cobalt, and zinc from water by a
602 cancrinite-type zeolite synthesized from fly ash. *Chem. Eng. J.* 145(3), 483-488.

603 Rios, C.A., Williams, C.D., Roberts, C.L., 2008. Removal of heavy metals from acid mine
604 drainage (AMD) using coal fly ash, natural clinker and synthetic zeolites. *J. Hazard. Mater.*
605 156(1-3), 23-35.

606 Santiago, O., Walsh, K., Kele, B., Gardner, E., Chapman, J., 2016. Novel pre-treatment of
607 zeolite materials for the removal of sodium ions: potential materials for coal seam gas co-
608 produced wastewater. *Springerplus* 5, 571.

609 Sprynskyy, M., Buszewski, B., Terzyk, A.P., Namiesnik, J., 2006. Study of the selection
610 mechanism of heavy metal (Pb^{2+} , Cu^{2+} , Ni^{2+} , and Cd^{2+}) adsorption on clinoptilolite. *J. Colloid*
611 *Interface Sci.* 304(1), 21-28.

612 Taffarel, S.R., Rubio, J., 2010. Adsorption of sodium dodecyl benzene sulfonate from
613 aqueous solution using a modified natural zeolite with CTAB. *Miner. Eng.* 23(10), 771-779.

614 Tolonen, E.-T., Sarpola, A., Hu, T., Rämö, J., Lassi, U., 2014. Acid mine drainage treatment
615 using by-products from quicklime manufacturing as neutralization chemicals. *Chemosphere*
616 117, 419-424.

617 Tomaszewska, M., Gryta, M., Morawski, A.W., 2001. Recovery of hydrochloric acid from
618 metal pickling solutions by membrane distillation. *Sep. Purif. Technol.* 22-23, 591-600.

619 Tomaszewska, M., Mientka, A., 2009. Separation of HCl from HCl–H₂SO₄ solutions by
620 membrane distillation. *Desalination* 240(1), 244-250.

621 Turner, M.D., Laurence, R.L., Conner, W.C., Yngvesson, K.S., 2000. Microwave radiation's
622 influence on sorption and competitive sorption in zeolites. *AIChE J.* 46(4), 758-768.

623 Unger, C., Lechner, A.M., Glenn, V., Edraki, M., Mulligan, D.R., 2012. Mapping and
624 Prioritising Rehabilitation of Abandoned Mines in Australia. *Proceedings Life of mine*
625 *conference, Brisbane, QLD, 259-265.*

626 Vasquez, Y., Escobar, M.C., Neculita, C.M., Arbeli, Z., Roldan, F., 2016. Biochemical
627 passive reactors for treatment of acid mine drainage: Effect of hydraulic retention time on
628 changes in efficiency, composition of reactive mixture, and microbial activity. *Chemosphere*
629 153, 244-253.

630 Vital, B., Bartacek, J., Ortega-Bravo, J.C., Jeison, D., 2018. Treatment of acid mine drainage
631 by forward osmosis: Heavy metal rejection and reverse flux of draw solution constituents.
632 *Chem. Eng. J.* 332, 85-91.

633 Wingenfelder, U., Hansen, C., Furrer, G., Schulin, R., 2005. Removal of Heavy Metals from
634 Mine Waters by Natural Zeolites. *Environ. Sci. Technol.* 39(12), 4606-4613.

635 Yao, M., Woo, Y.C., Tijing, L.D., Choi, J.-S., Shon, H.K., 2018. Effects of volatile organic
636 compounds on water recovery from produced water via vacuum membrane distillation.
637 *Desalination* 440, 146-155.

638 Zhang, M., 2011. Adsorption study of Pb(II), Cu(II) and Zn(II) from simulated acid mine
639 drainage using dairy manure compost. *Chem. Eng. J.* 172(1), 361-368.

640

641

Supplementary Material

[Click here to download Supplementary Material: Supplementary document.doc](#)